Topic

Date March 2020

Stationary unconfined fluids

→ normal forces acting on a fluid element arise entirely from the weight of the fluid column above

↳ Study of statics — fluid statics

Equations governing forces acting on objects submerged in a stationary fluid obtained from the principles

$$\Sigma F = 0$$
(Summation of forces)

$$\Sigma H = 0$$
(Summation of moments)

→ Fluid Dynamics — study of fluids in motion

Physical principles which determine governing fluid flow are:

→ Conservation of mass
→ Newton's second law of motion

→ Various aspects of fluid motion without being concerned with the actual forces necessary to produce the motion

Kinematics of motion — Velocity & acceleration

↳ Visualization of motion

VFT Lecture 3



Topic _____ Date March 2020

→ Fluid mechanics is a highly visual subject

→ patterns of flow can be visualized in a dozen different ways

→ four basic types of line patterns are used to visualize flows

→ streamline — is a line everywhere tangent to the velocity vector at a given instant

→ pathline — is the actual path traversed by a given fluid particle

→ streakline — is the locus of particles that have earlier passed through a prescribed point

→ timeline — is a set of fluid particles that form a line at a given instant

→ streamline — calculated mathematically

→ pathline, streakline & timeline — determined experimentally

In steady flows streamlines, pathlines and streaklines are identical

Topic _____ Date March 2020

→ Wide variety of useful info can be gained from a thorough understanding of fluid kinematics

Visualizations
- → smoke issuing thru the chimneys
- → motion of waves
- → mixing of paints

Some methods of flow visualization are:

i) Dye, smoke or bubble discharges
ii) Surface powder or flakes on liquid flows
iii) floating or natural-density particles
iv) Optical techniques that detect density changes in gas flows:
- → shadowgraphy
- → schlieren

and → interferometer

v) Tufts of yarn attached to boundary surfaces
vi) Evaporative coatings on boundary surfaces
vii) Luminescent fluids, additives or bioluminescence
viii) Particle image Velocimetry (PIV)

Topic _____ Date March 2020

## Velocity field

→ field representation of the flow

Temperature, $T = T(x, y, z, t)$

$x, y, z$ — Space — Spatial

$t$ — Time — temporal

Likewise

Velocity, $V = V(x, y, z, t)$

$$V = u(x,y,z,t)\hat{i} + v(x,y,z,t)\hat{j} + w(x,y,z,t)\hat{k}$$

$u$ → $x$
$v$ → $y$
$w$ → $z$

} components of Velocity

$$|V| = \left(u^2 + v^2 + w^2\right)^{1/2}$$

Acceleration may be due to change in speed/and or direction

Topic _____ Date March 2020

## Eulerian & Langrangian flow description

### Langrangian

→ fluid motion is described by tracing the kinematic behavior of each & every individual particle constituting the flow

### Eulerian

→ avoids determination of the movement of each individual particles in all details

→ instead it seeks the velocity and other details, its variation with time at each and every location in the flow field

Ex

→ a temperature measuring device may be fixed to the top of the chimney

→ will record temperature at that point as a function of time

$$T(x, y, z, t)$$

→ Use numerous such measuring devices will give full temperature field.

$$T(x, y, z, t)$$

Unlike this in Langrangian approach — one would attach the temperature measuring device to a particular fluid particle and record the particle temperature as it moves about

Topic _____ Date March 2020

## Classification of Fluid flows

→ There is a wide variety of fluid flow problems encountered in practice

→ it is usually convenient to classify them on the basis of some common characteristics to make it feasible to study them in groups

→ Many ways to classify fluid flow problems

Some general categories

→ Viscous Verus Inviscid regions of flow

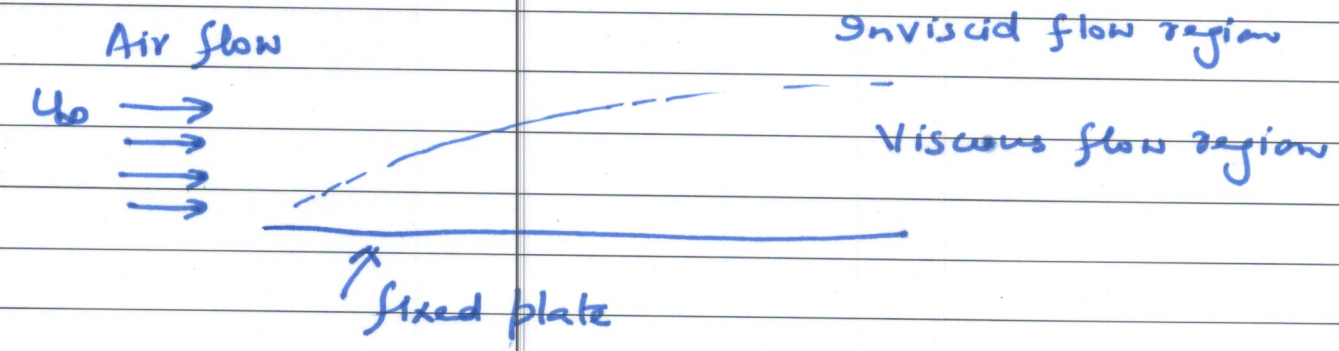


→ Internal Verus External flow

→ flow of an unbounded fluid over a surface such as plate, a wire, or a pipe — external flow

→ flow in a pipe or duct — fluid is completely bounded by solid surfaces — internal flow

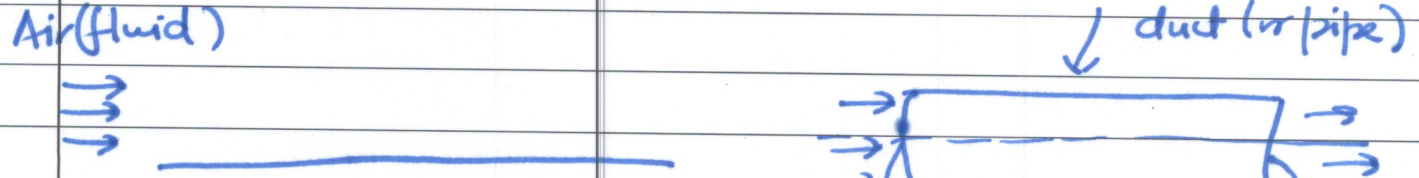

Topic _____ Date March 2020

## Compressible Versus Incompressible flow

→ Depends on the level of variation of density during flow

→ Incompressibility is an approximation — if density remains nearly constant throughout

→ Volume of every portion of fluid remains unchanged over the course of its motion for incompressible approximation

→ When analyzing rockets, space crafts and other systems that involve high speed gas flows, the flow speed is often expressed in terms of dimensionless Mach number

$$\text{Mach number, } Ma = \frac{\text{Speed of flow}}{\text{Speed of sound}} = \frac{U}{c}$$

speed of sound, c is 340 m/s in air at room temperature

→ flow is sonic when $Ma = 1$

subsonic when $Ma < 1$

supersonic when $Ma > 1$

Hypersonic $Ma \gg 1$

→ Liquid flows are incompressible to a high level of accuracy

→ level of variation of density in gas flows and consequent level of approximation depends on Mach number

→ Gas flows can be approximated as incompressible if the density changes are under 5% which is usually when $Ma < 0.3$

Compressibility effects of air at room temperature

March 2020

Topic _____ Date _____

## Laminar Verus Turbulent flow

Laminar — smooth, regular, highly ordered, deterministic

Turbulent — irregular, highly disordered, fluctuations

Ex — flow of high viscosity fluids such as oils at low velocities — laminar

— flow of low viscosity fluids such as air at high velocities — turbulent

## Natural (or unforced) Verus Forced flow

→ fluid forced over a surface or in a pipe by external means such as pump or a fan → forced flow

→ fluid motion due to natural means such as buoyancy effects (manifests itself as the rise of warmer lighter fluid and the fall of cooler denser fluid

Ex Solar hot-water systems — thermosiphoning effect is commonly used to replace pumps by placing the water tank sufficiently above the solar collectors

Topic _____ Date March 2020

## Steady Versus Unsteady Flow

Steady → implies no change of properties velocity, temperature, etc at a point with time.

uniform → implies no change with location over a specified region

unsteady & transient
?
flow that is not steady } used for developing flows

periodic ~ refers to kind of unsteady flow in which the flow oscillates about a steady mean

→ Steady-flow conditions can be closely approximated by devices that are intended for continuous operation such as turbines, pumps, boilers, condensers, & heat exchangers of power plants or refrigeration systems

→ Some cyclic devices such as reciprocating engines or compressors don't satisfy the steady-flow conditions since the flow at the inlets and the exits is pulsating and not steady

→ fluid properties vary with time in a periodic manner and the flow thru these devices can still be analyzed as a steady-flow process by using time-averaged values

Topic _____ Date March 2020

## One-, Two-, and Three-Dimensional Flows

→ flow field is best characterized by its velocity distribution

One - D
Two - D
Three - D
} flows

if flow velocity varies in one, two or three primary dimensions

3D flow $\vec{V}(x, y, z)$ → rectangular
$\vec{V}(r, \theta, z)$ → cylindrical
} coordinates

Variation of velocity in certain directions can be small relative to the variation in other directions and can be ignored with negligible error

→ flow can be modeled as being

One - dimensional
or Two - dimensional

which } are easier to analyze

# FLOW VISUALIZATIONS

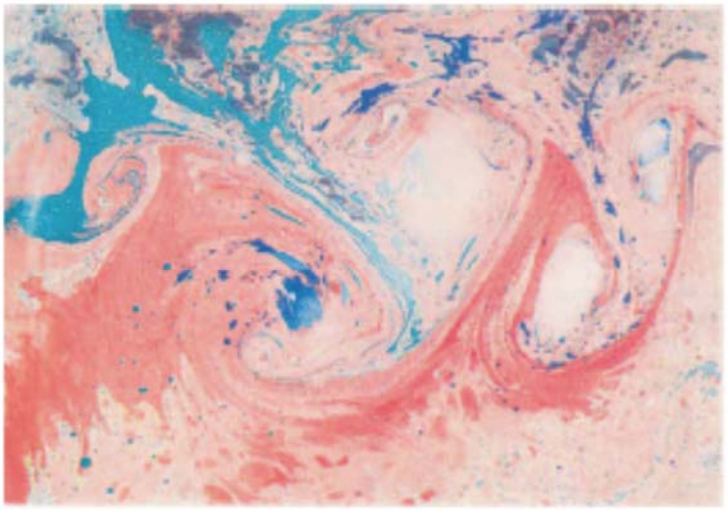

Figure 1

Figure 2

# Vortex flows paint themselves

G. E. Koppenwallner and D. Etling

*Universität of Hannover, Germany*

The artistitke pictures of vortex flows presented here have been produced by the flow itself. The method of this "natural" flow visualtzation can be described briefly as follows: The working fluid ts water mtxed with some paste tn order to tncrease the vtscostty. Vortex flows are produced by pulltng a stick or stmtlar devtces through the fluid or by tnjectting fluid through a nozzle tnto the working tank.

The flow vtsualtzation ts performed tn the followtng way: the surface of the fluid at rest ts sparkled with otl paint of different colors dtluted wtth some evaporattng chemtcal. After the vortex structures have formed due to wakes or jets, a sheet of white paper ts placed on the surface of the working fluid, where the otl color ts attached to the paper tmmediately. The final results are artistitke paintings of vortex flows which exhtbtt a rtch vartety of flow structures.

**Keywords**

oil paint visualization; direct image-transfer.

Figure 1 Photograph of *Naruto* taken from a Yomiuri Shimbun helicopter during early March, 1996, by Masafumi Nanjo of the *Daily Yomiuri*, Tokyo, Japan.

# Naruto: past and present*

Norman J. Zabusky and Wesley Townsend

*Laboratory for Visiometrics and Modeling*
*Rutgers University*

**Keywords**

maelstrom; whirlpool; tidal vortex.

The Naruto strait contains a tidal current whose edges constitute a gigantic cascading "maelstrom." It is not far from Kobe, Japan and lies between the city of Naruto on Shikoku Island and the island of Awaji (Hyogo Prefecture) and connects the higher Seto Inland Sea (Setonaikai) and the lower Osaka Bay.[1] The rushing tidal current is a sloping surface jet (exceeding 5 m/s) in-or-out between the two seas. The phenomenon is strongest during the first hour of every 6 h and 25 min period, particularly at full moons in the early spring, when Nanjo's photograph was taken (early March, 1996). A bridge now spans Naruto to Awaji and was finished in March of 1985.

In the photograph we see a near-vertical aerial view of a sight-seeing boat close to the southwestern (counter-clockwise-vortex) edge of the cascade. Dominant vortex structures may be 30 m in diameter. We await the quantification of the stratified turbulence of this natural wave-vortex system.

* This page summarizes the Naruto images collected by N. J. Zabusky during his visit to Japan in 1996. The photograph above was provided by Masafumi Nanjo of the Daily Yomiuri, Tokyo, Japan and is printed with his permission. The photograph was submitted as the poster, "Naruto '96" to the 1996 Gallery of Fluid Motion at the American Physical Society Division of Fluid Dynamics annual meeting in November, 1996. Another submission was a video "NARUTO: Past and Present," created by Norman J. Zabusky and Wesley Townsend. It was based on the 19th-century Ukiyo-e print by Ando Hiroshige and an NHK Tokushima video made during the bridges inauguration ceremony in March of 1985 and Nanjo's print. The video was provided by Professor K. Ishii of the Department of Applied Physics at Nagoya University. N. J. Zabusky acknowledges the gift of these images. Many of them can be seen on our URL home page, http://caip.rutgers.edu/vizlab.naruto.html

[1] For sightseeing information, see Jay Gluck, Sumi Gluck, and Garet Gluck, *Japan Inside Out* (Personally Oriented, Ltd., Ashiya, Japan, 1992).

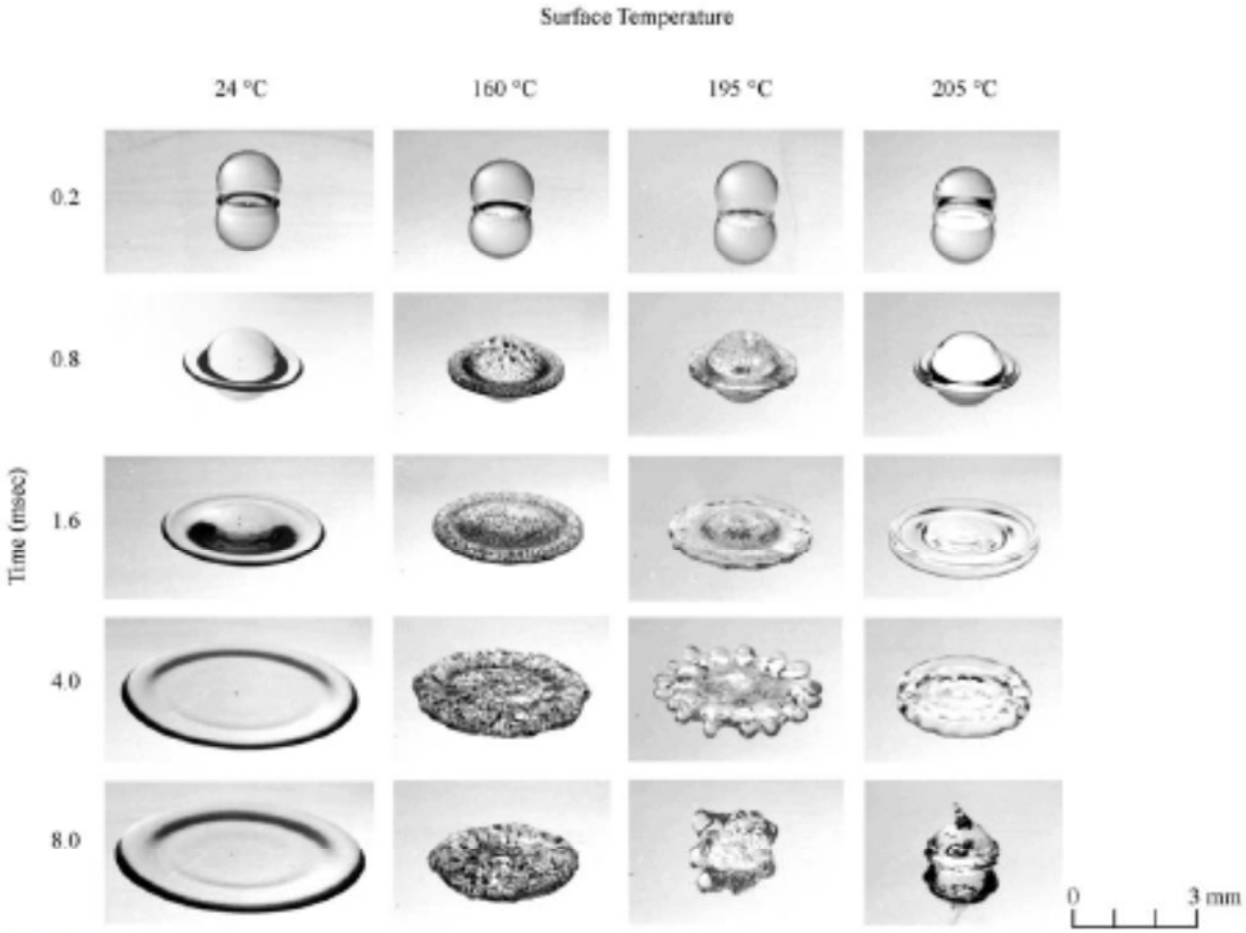


Figure 1

# The collision of a droplet with a solid surface

S. Chandra and C. T. Avedisian

*Cornell University*

The photographs displayed above show the impact, spreading, and boiling history of *n*-heptane droplets on a stainless steel surface. The impact velocity, Weber number, and initial droplet diameter are constant (values of 1 m/s, 43 and 1.5 mm respectively), and the view is looking down on the surface at an angle of about 30°. The photographs were taken using a spark flash method[1] and the flash duration was 0.5 μs. The dynamic behavior illustrated in the photographs is a consequence of varying the initial surface temperature.

The effect of surface temperature on droplet shape may be seen by reading across any row; the evolution of droplet shape at various temperatures may be seen by reading down any column. An entrapped air bubble can be seen in the drop when the surface temperature is 24°C. At higher temperatures vigorous bubbling, rather like that of a droplet sizzling on a frying pan, is seen (the boiling point of *n*-heptane is 98°C) but the bubbles disappear as the Leidenfrost temperature of *n*-heptane (about 200°C) is exceeded because the droplet become levitated above a cushion of its own vapor and does not make direct contact with the surface. The droplet shape is unaffected by surface temperature in the early stage of the impact process ($t \leq 0.8$ ms) but is affected by temperature at later time (cf. $t \geq 1.6$ ms) because of the progressive influence of intermittent solid–liquid contact as temperature is increased.

**Keywords**

cavitation bubble; Leidenfrost effect; surface tension.

[1] S. Chandra and C. T. Avedisian, "On the collision of a droplet with a solid surface," *Proceedings of the Royal Society of London* A **432**, 13–41 (1991).

Figure 1(a)

Figure 1(b)

Figure 1(c)

Figure 1(d)

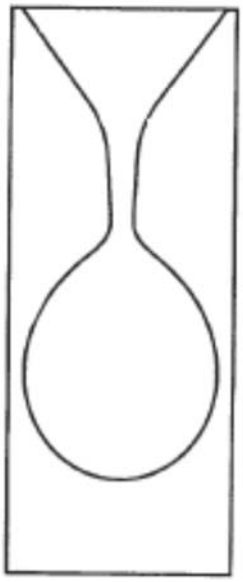

Figure 2(a)

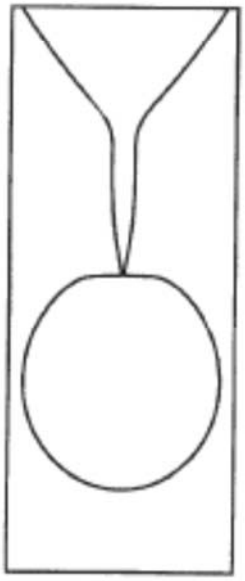

Figure 2(b)

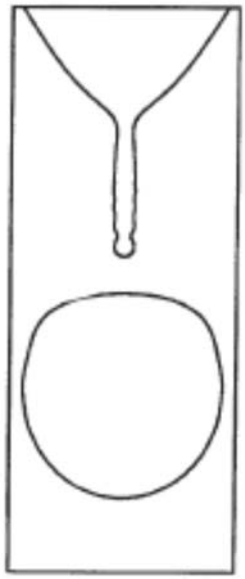

Figure 2(c)

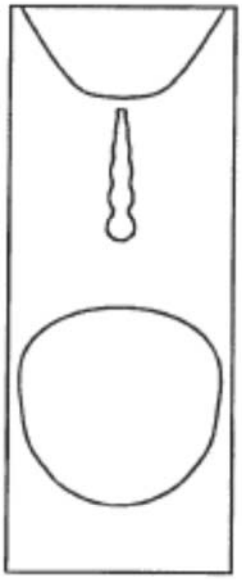

Figure 2(d)

# The bifurcation of liquid drops

Michael P. Brenner, X. D. Shi, Jens Eggers, and Sidney R. Nagel

*Massachusetts Institute of Technology*

**Keywords**

surface tension; dripping faucet; droplet pinchoff; simulation and experiment.

The breakup of fluid drops is one of the simplest and most ordinary examples of a hydrodynamic singularity, in which physical quantities diverge in a finite amount of time. These pictures document our experiments and computer simulations of a water drop falling from a nozzle.[1,2]

In the top panel we show a sequence of photographs in which the drop first breaks at the bottom and then near the nozzle. The second row shows a numerical simulation of the process using modified long-wavelength equations.[3]

[1] X. D. Shi, M. P. Brenner, and S. R. Nagel, "Cascade of structure in a drop falling from a faucet," *Science* **265**, 219 (1994).

[2] M. P. Brenner, J. Eggers, K. Joseph, S. R. Nagel, and X. D. Shi, "Breakdown of scaling in droplet fission at high Reynolds number," *Phys. Fluids* **9**, 1573 (1997).

[3] J. Eggers and T. F. Dupont, "Drop formation in a one-dimensional approximation of the Navier–Stokes equation," *J. Fluid Mech.* **262**, 205 (1994).

Figure 1

Figure 2

# Water balloon rupture in low-g

M. M. Weislogel

*NASA Lewis Research Center*

and S. Lichter

*Northwestern University*

A qualitative study of the bursting of water balloons in a simulated low-gravity environment was conducted aboard NASA Lewis's DC-9 aircraft. Following rupture by a syringe needle, the balloon retracts tangent to the water surface leaving a smooth surface near the puncture location, Fig. 1. Asymmetries soon develop as the membrane rips apart, ejecting a directional spray from the surface. When the balloon parts from the drop entirely, it causes a large deformation of the remaining liquid mass leading to significantly underdamped oscillations which persist for the duration of the simulation.

In Fig. 2 an approximately 2.5 liter blob of undulating water hovers after rupture of the membrane. A free floating, red-dyed water blob flattens, crowns, and breaks up after impact by an impinging blue-dyed water jet, Fig. 3. In Fig. 4 a large air bubble is blown into a free floating blob using a straw. Such flows are *unearthly* in that a balance is struck between capillary and inertial forces over truly large length scales.

The tests were performed to develop techniques to rapidly deploy large liquid drops in a microgravity environment. The footage has also proven of general interest and is used to introduce students to low-g phenomena. Quicktime movies may be found at http://zeta.lerc.nasa.gov/balloon/blob.htm. Related ground tests were also performed using high-speed video photography and may be found at http://zeta.lerc.nasa.gov/balloon/hs.htm.

Figure 3

Figure 4

**Keywords**

capillary wave; inertial oscillations; capillary length-scale.

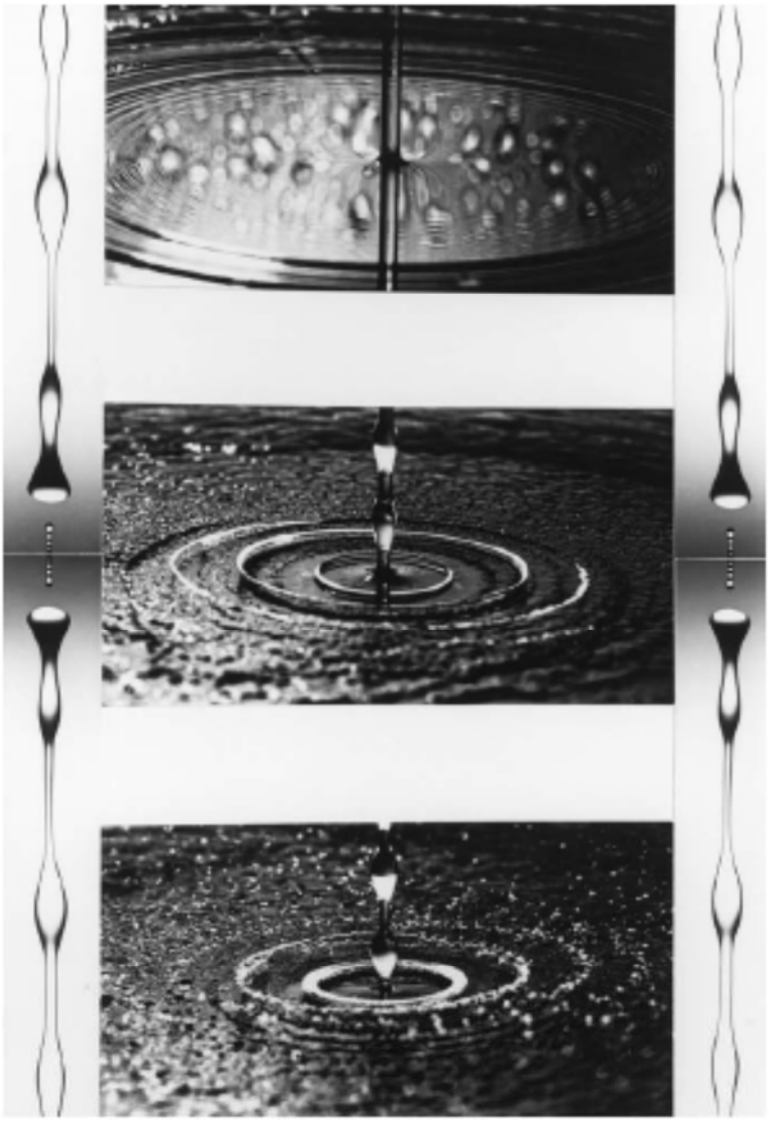

Figure 1

## Laminar jets can splash!

Mario Errico

*University of California at San Diego*

It has been observed that a liquid jet impinging on a solid surface can produce splashing. High-speed photography has revealed that, with a turbulent jet, splashing is related to the jet surface roughness. To investigate the importance of the jet shape on splashing, perturbations of known frequency or amplitude are imposed on the surface of a smooth laminar jet.

The top picture shows the unperturbed smooth jet as it spreads radially on the solid surface. The varicose deformations imposed on the jet surface alter the flow quite dramatically (center picture). As we further increase the amplitude of the oscillations, splashing starts suddenly. The bottom picture shows the beauty and complexity of splashing.

**Keywords**

forced jet; atomization; jet impingement.

Figure 1 Re = $O$ (HUNDRED)

Figure 2 Re = $O$ (BILLION?) "BIG ENOUGH"

## Atom bomb / water drop

Lorenz Sigurdson

*University of Alberta*

On the right, an aboveground nuclear test in Nevada in 1957 (US Department of Energy).

On the left a water drop falling into a pool of clear water (photo inverted, drop dyed with fluorescein, photo taken by Peck and Sigurdson[1]).

The similarity in large-scale structure is despite a tremendous difference in Reynolds number and buoyancy effects.

The hypothesized vortex skeleton structure[1,2] is represented by three closed vortex lines: the primary ring with four azimuthal waves, four connected loops "shedding" from the ring, and four counter-rotating vortex pairs forming a "stalk" reaching from the primary ring to another ring of opposite sign situated at the bounding surface.

The reasons for the similarity in structure involve the initial conditions for the vorticity generation. The bomb shortly after detonation consists of a fireball and vorticity is generated at its surface. It is produced from pressure gradients acting on the density gradient between the less dense fireball and the nearby air. The pressure gradients consist of the vertical hydrostatic pressure gradient and the pressure gradient associated with the shock wave which is reflected upward from the ground.

The vorticity generation mechanism for the water drop has been an area of investigation.[1,3]

[1] B. Peck and L. Sigurdson, "The three-dimensional vortex structure of an impacting water drop," *Phys. Fluids* **6** (2), 564–576 (1994); L. Sigurdson, "Flow visualization in turbulent large-scale structure research," *Flow Vis. Soc., Japan, Atlas of Visualization*, **3**, 99–113 (1997).

[2] L. Sigurdson, *Bull. Am. Phys. Soc.* **32**, 2095 (1987).

[3] L. Sigurdson and B. Peck, *Bull. Am. Phys. Soc.* **34**, 2286 (1989).

**Keywords**

mushroom vortex.

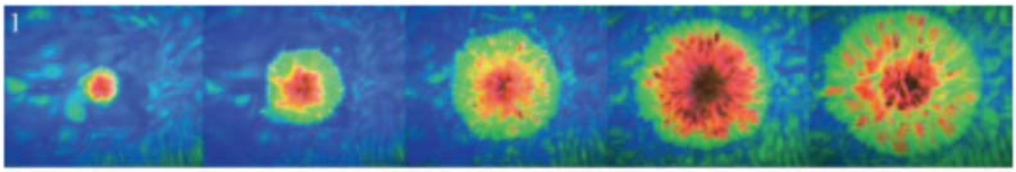


Figure 1

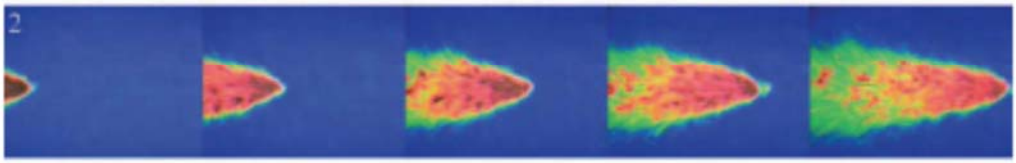


Figure 2

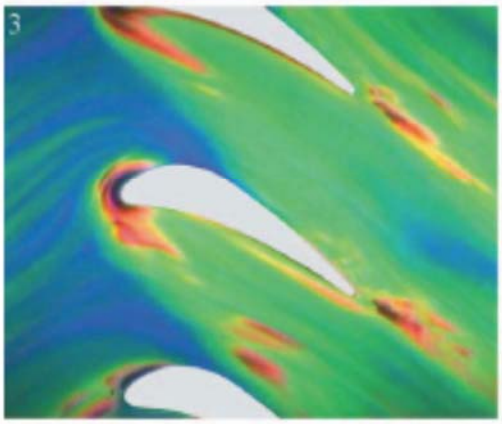


Figure 3 (left)

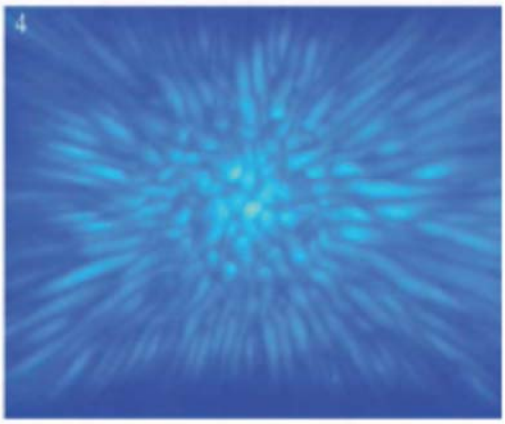


Figure 4 (right)

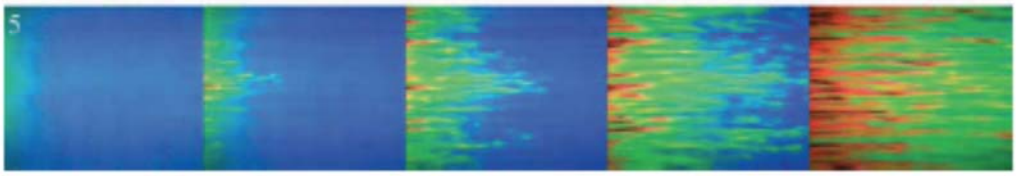


Figure 5

## The colors of turbulence

D. R. Sabatino and T. J. Praisner

*Lehigh University*

Thermochromic Liquid Crystals (TLCs) possess unique physical properties which make them a powerful tool for temperature visualizations/measurements. The images above illustrate a variety of turbulent flows for which surface heat transfer is reflected by the color change of TLCs applied to a unique thin-film constant heat flux surface. All of the images display color patterns which are proportional to the instantaneous convective coefficients.

Figure 1 illustrates the surface heat transfer patterns for a jet of cool fluid impinging onto a warm surface. Figure 2 shows a temporal sequence of patterns generated by a passing turbulent jet of cool fluid. Instantaneous end-wall temperature distributions at the base of a turbine cascade are illustrated in Figure 3. Figure 4 illustrates patterns created by free-convection cells distorted by a sink above the center of the heated plate. Finally, the sequence shown in Figure 5 shows the transition of a laminar to a fully turbulent boundary layer, as illustrated by the development of the classic low-speed streak patterns.

While TLC thermography is a useful visualization technique, it is even more valuable as a quantitative sensor of surface heat transfer. Employing a unique experimental apparatus, TLC measurements have been simultaneously combined with high resolution PIV to yield quasi-three-dimensional results. To see details of this technique and selected results, visit www.lehigh.edu/fluid.

**Keywords**

thermochromic liquid crystals; turbine cascade; heat-transfer patterns.

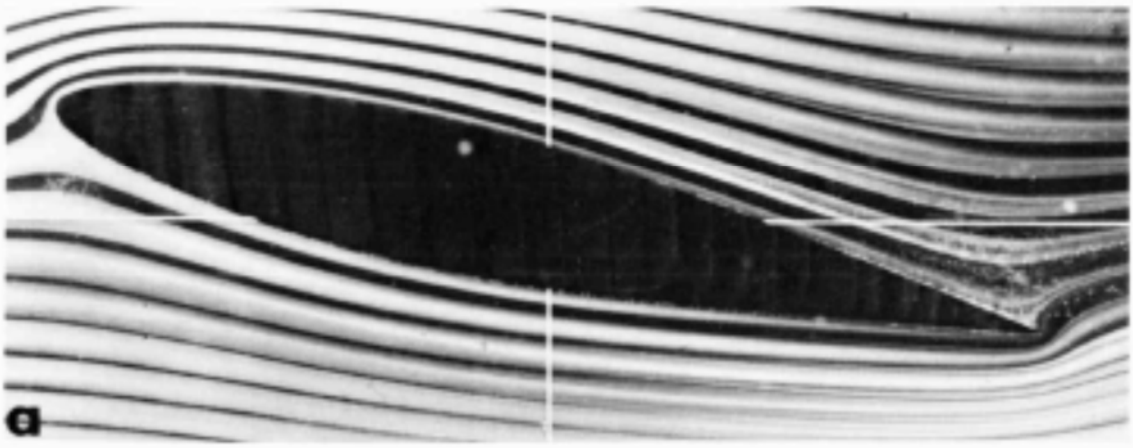

**4. Hele-Shaw flow past an inclined airfoil.** Dye in oil shows the streamlines of plane potential flow past an NACA 64A015 airfoil at 13° angle of attack. However, because the Hele-Shaw flow cannot show circulation, the Kutta condition is not enforced at the trailing edge. Hence infinite velocities are represented there. The model is between glass plates 1 mm apart. *Werlé 1973. Reproduced, with permission, from the Annual Review of Fluid Mechanics, Volume 5.* 

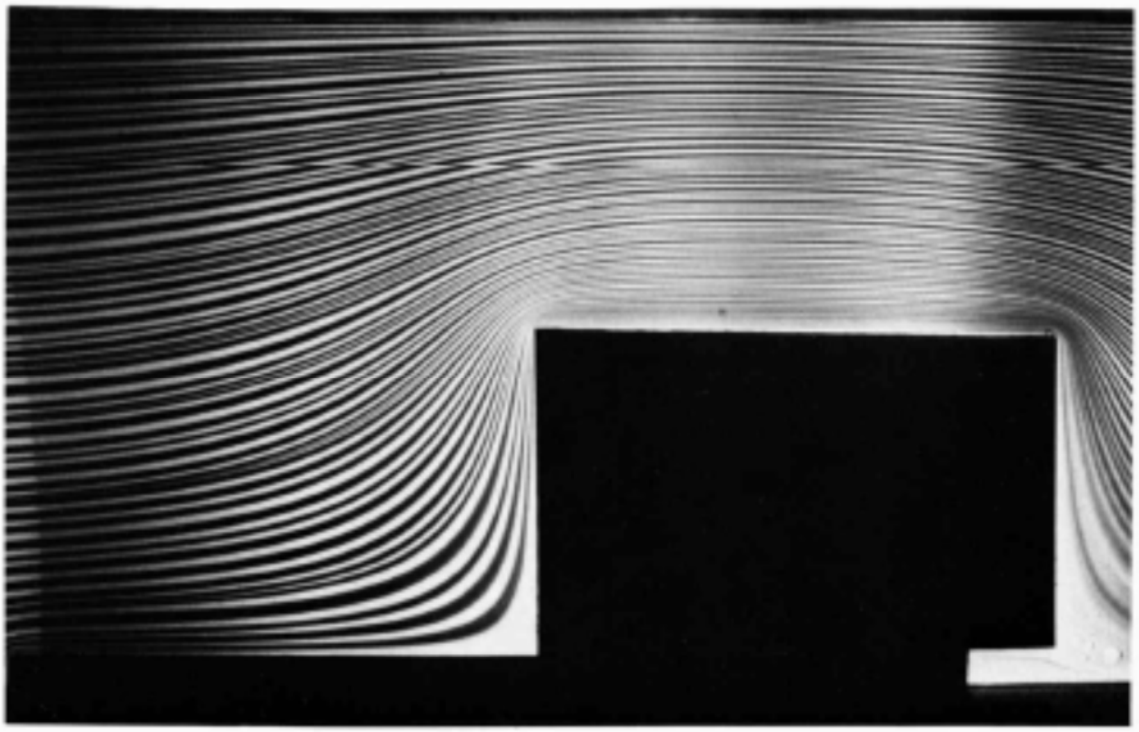

**5. Hele-Shaw flow past a rectangular block on a plate.** The analogy faithfully simulates the unseparated potential flow into the stagnation region of a concave corner, and the infinite velocities over an outside corner. The water takes much longer to travel through the system if it follows a streamline that passes close to a stagnation point. This allows a greater diffusion of dye, which is seen in the slight blurring of streamlines at the lower right-hand corner. *Photograph by D. H. Peregrine*

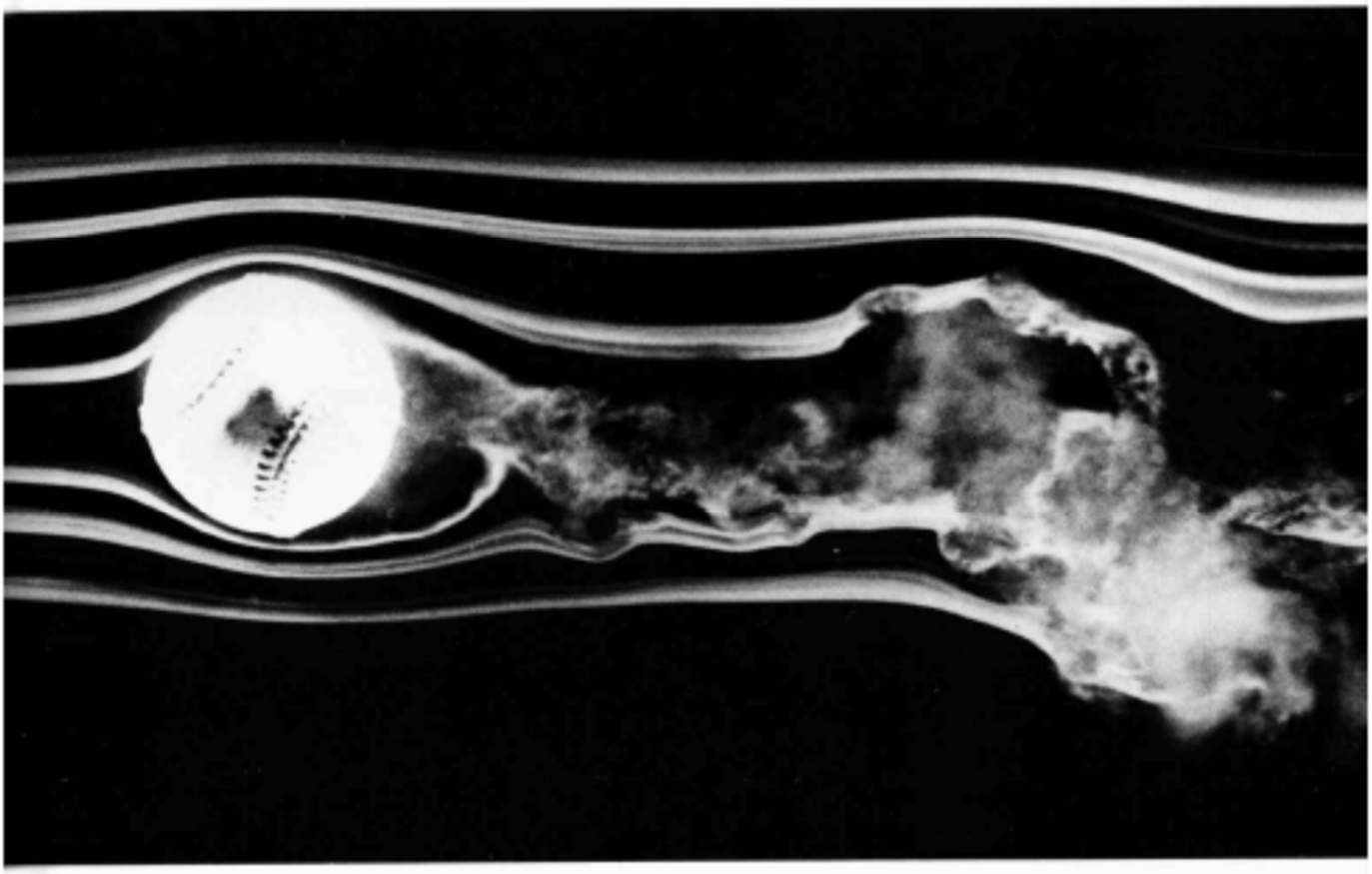

**66. Spinning baseball.** The late F. N. M. Brown devoted many years to developing and using smoke visualization in wind tunnels at the University of Notre Dame. Here the flow speed is about 77 ft/sec and the ball is rotated at 630 rpm. This unpublished photograph is similar to several in Brown 1971. *Photograph courtesy of T. J. Mueller*

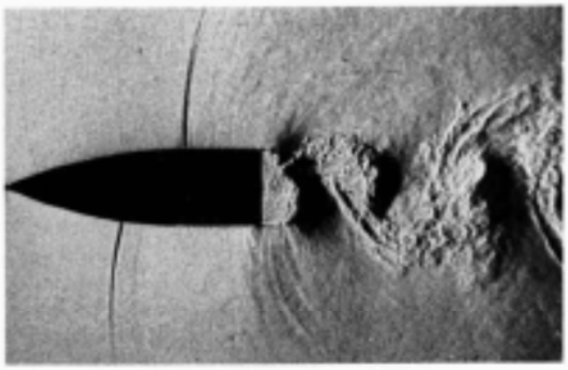

**67. Oscillating wake of a blunt-based airfoil.** At 0.6 Mach number and Reynolds number 220,000 a high-speed schlieren motion picture shows waves moving upstream alternately over each surface from a periodically oscillating wake. The separation is laminar at the base. *Dyment, Fiodrops & Gryson 1982*

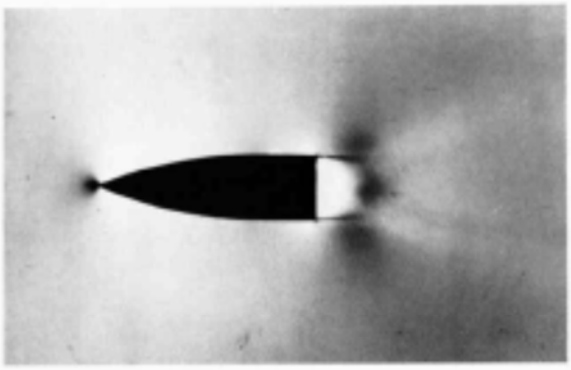

**68. Mean flow over a blunt-based airfoil.** A 1/400-second exposure averages the flow at the left over a dozen cycles to give a completely different impression of the motion. *Dyment & Gryson 1978*

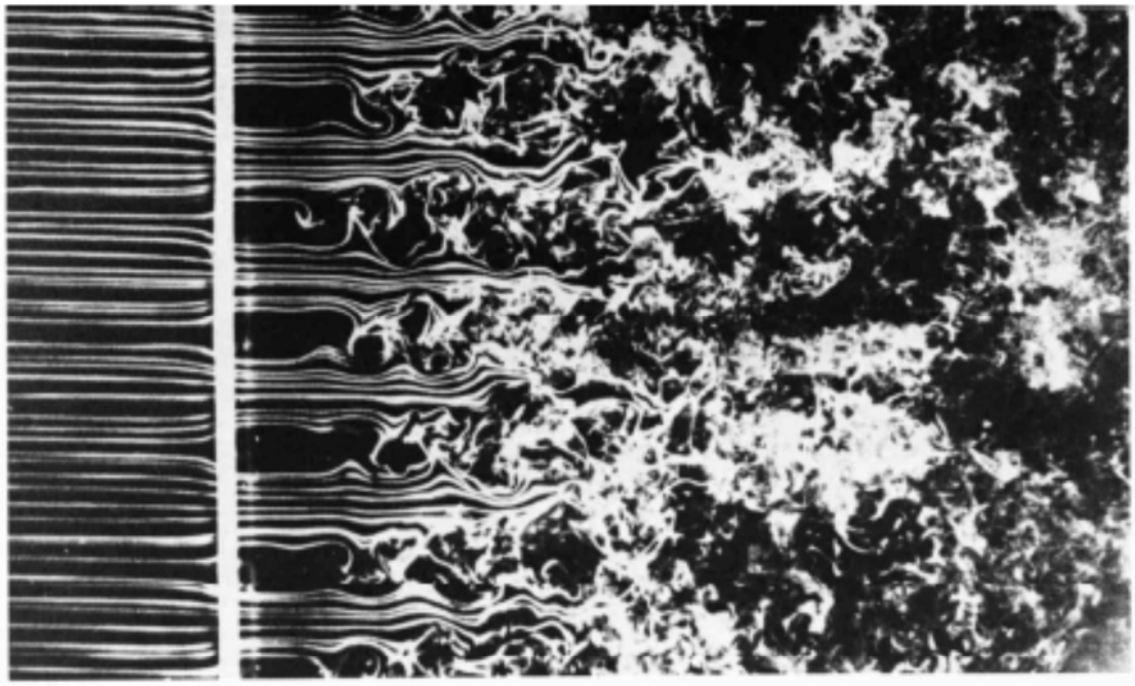

**152. Generation of turbulence by a grid.** Smoke wires show a uniform laminar stream passing through a $\frac{1}{16}$-inch plate with ¾-inch square perforations. The Reynolds number is 1500 based on the 1-inch mesh size. Instability of the shear layers leads to turbulent flow downstream. *Photograph by Thomas Corke and Hassan Nagib*

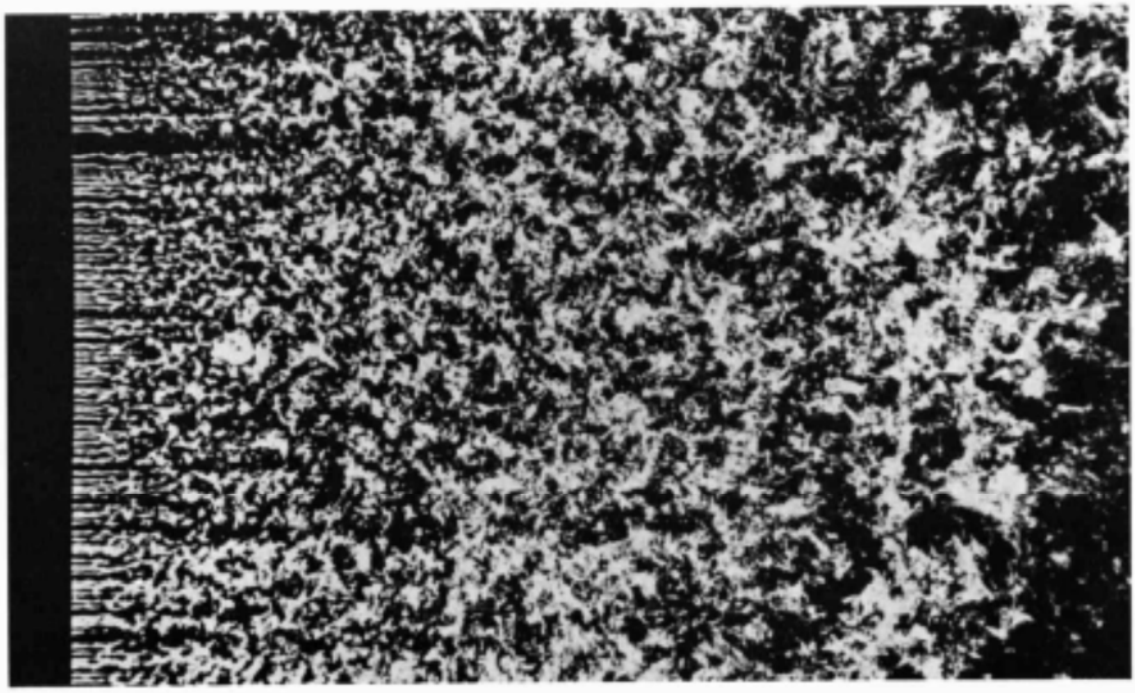

**153. Homogeneous turbulence behind a grid.** Behind a finer grid than above, the merging unstable wakes quickly form a homogeneous field. As it decays downstream, it provides a useful approximation to the idealization of isotropic turbulence. *Photograph by Thomas Corke and Hassan Nagib*

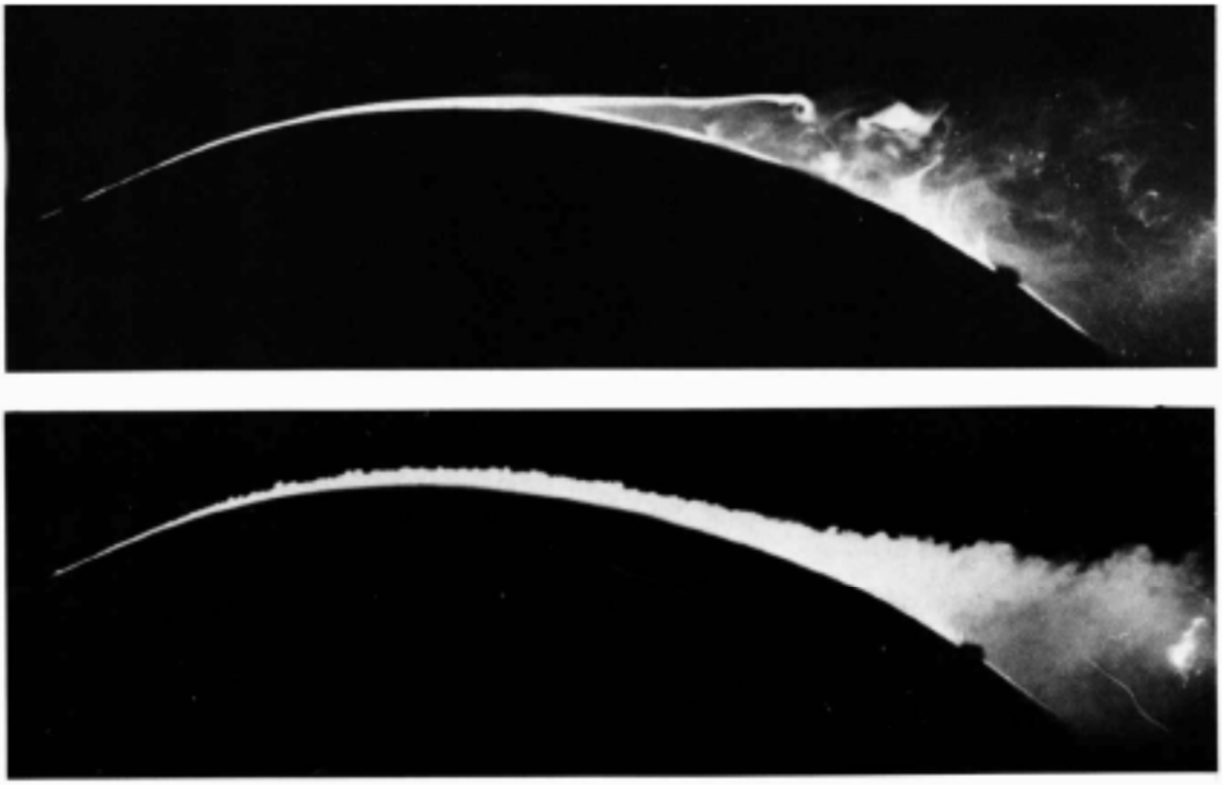

**156. Comparison of laminar and turbulent boundary layers.** The laminar boundary layer in the upper photograph separates from the crest of a convex surface (cf. figure 38), whereas the turbulent layer in the second photograph remains attached; similar behavior is shown below for a sharp corner. (Cf. figures 55-58 for a sphere.) Titanium tetrachloride is painted on the forepart of the model in a wind tunnel. *Head 1982*

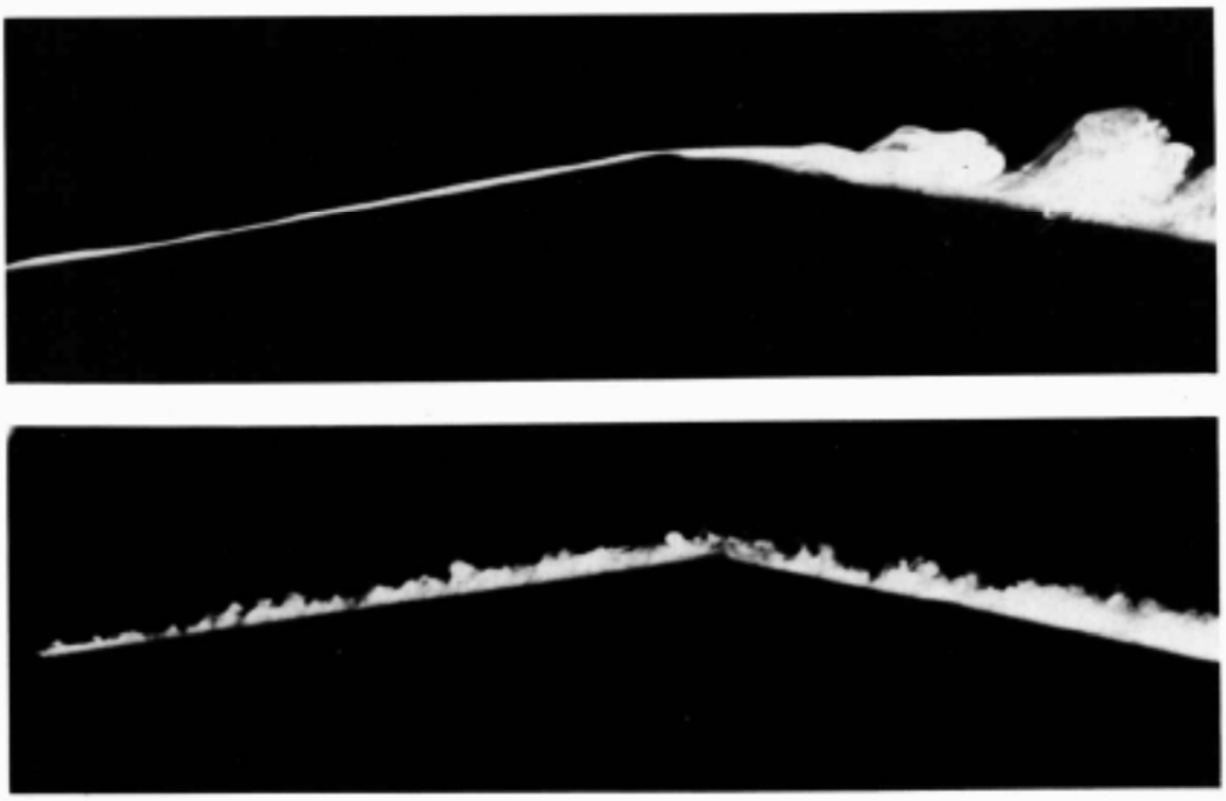

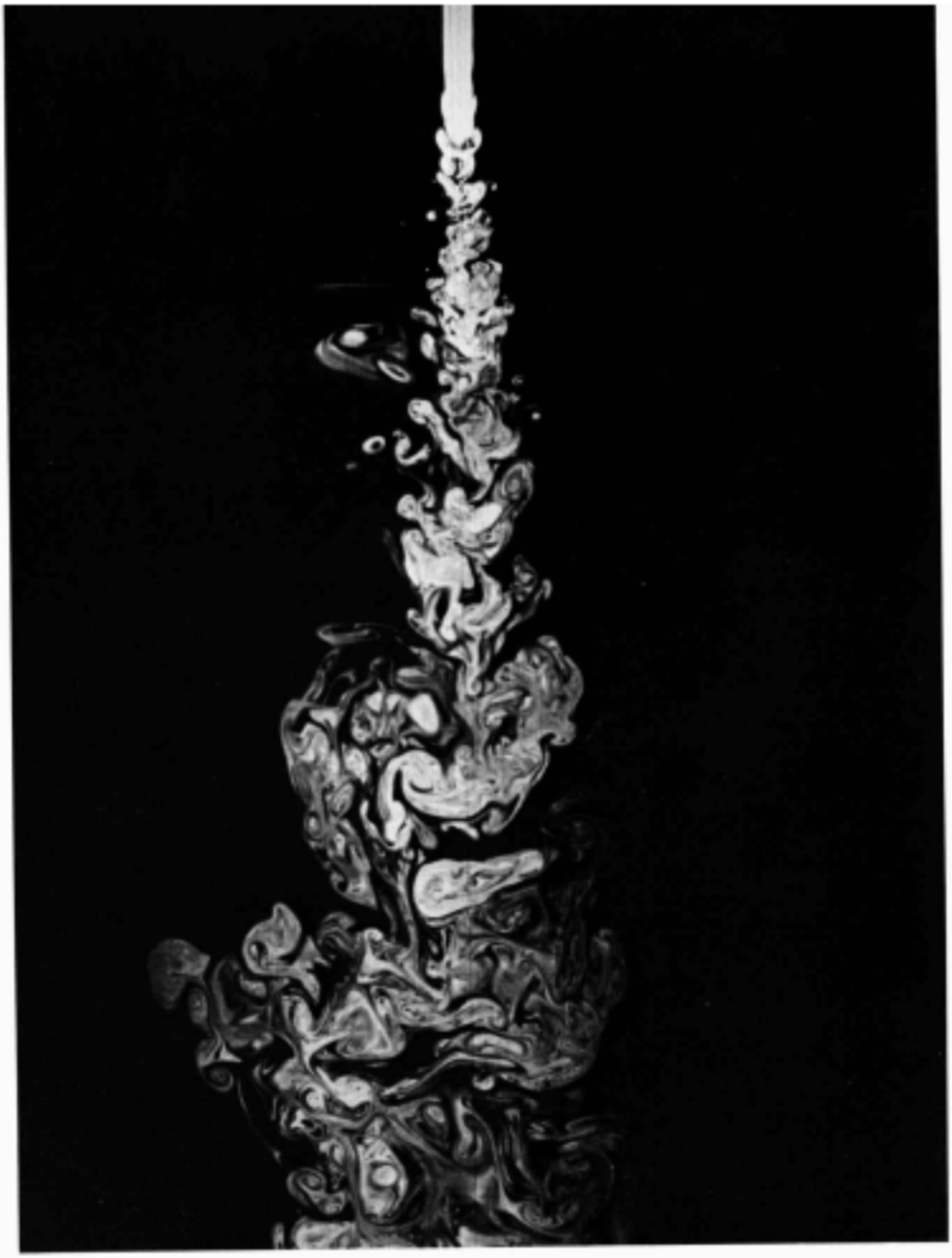

**166. Turbulent water jet.** Laser-induced fluorescence shows the concentration of jet fluid in the plane of symmetry of an axisymmetric jet of water directed downward into water. The Reynolds number is approximately 2300. The spatial resolution is adequate to resolve the Kolmogorov scale in the downstream half of the photograph. *Dimotakis, Lye & Papantoniou 1981*

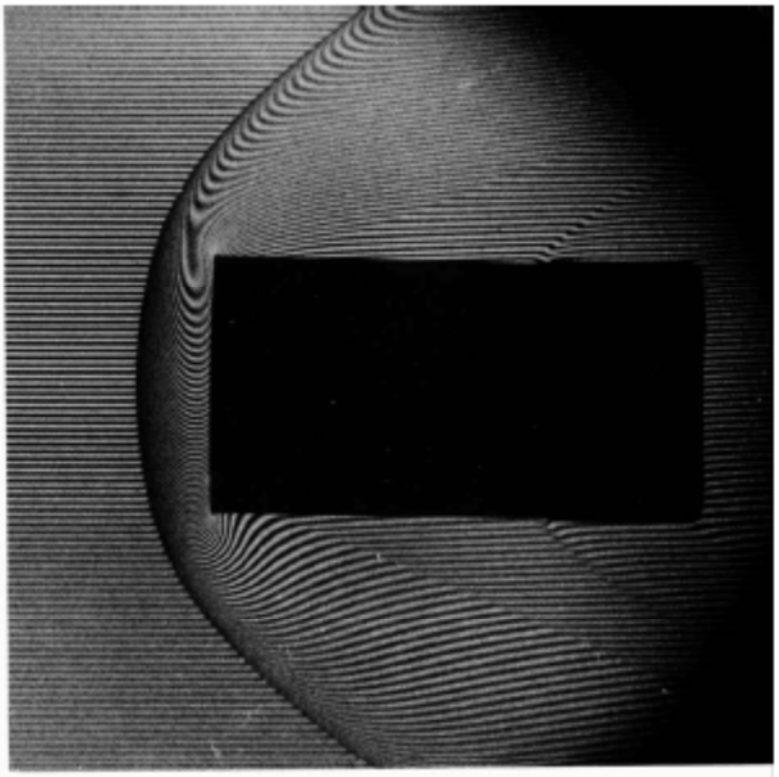

**264. Cylinder at M=2.77 in carbon dioxide.** A finite-fringe interferogram of a circular cylinder in free flight shows the bow wave wrapped more closely about the flat face than in the preceding photograph, both because the free-stream Mach number is greater and because the adiabatic exponent is lower, being 4/3 for carbon dioxide compared with 7/5 for air. The shock wave at reattachment is visible, followed by a second oblique shock wave from a bump on the cylinder. *Photograph from Air Flow Branch, U.S. Army Ballistic Research Laboratory*

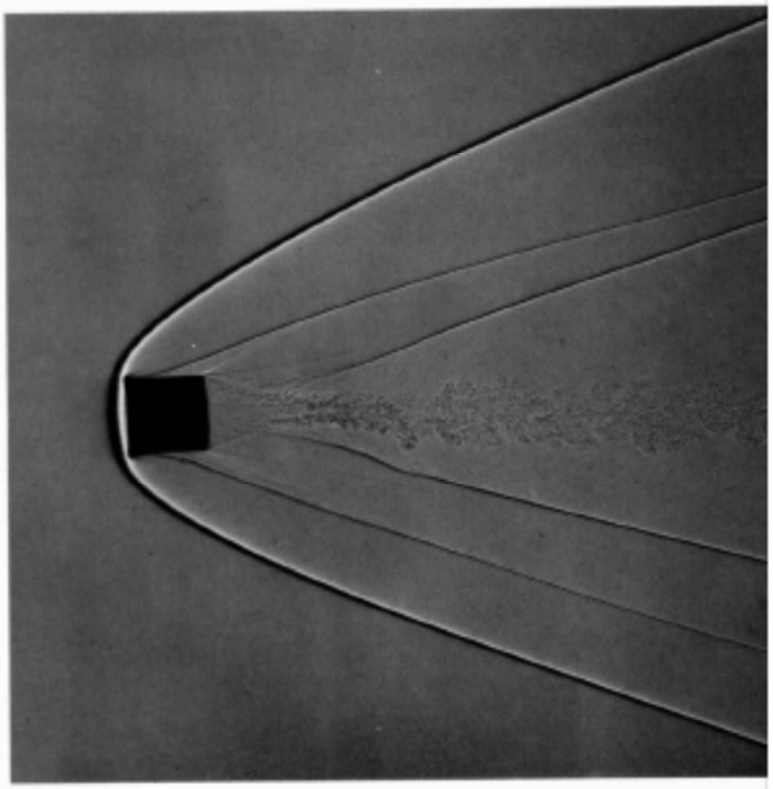

**265. Cylinder at M=3.6 in air.** A shadowgraph shows a circular cylinder in free flight at a small negative angle of attack. The apparent squashing of the face is actually optical distortion. The oblique shock wave from boundary-layer reattachment is seen merging with the wave from the wake. At great distances they form the rear of the N-wave pressure signature, shown for a sphere in figure 269, that is characteristic of any object in supersonic flight. *Photograph by A. C. Charters*

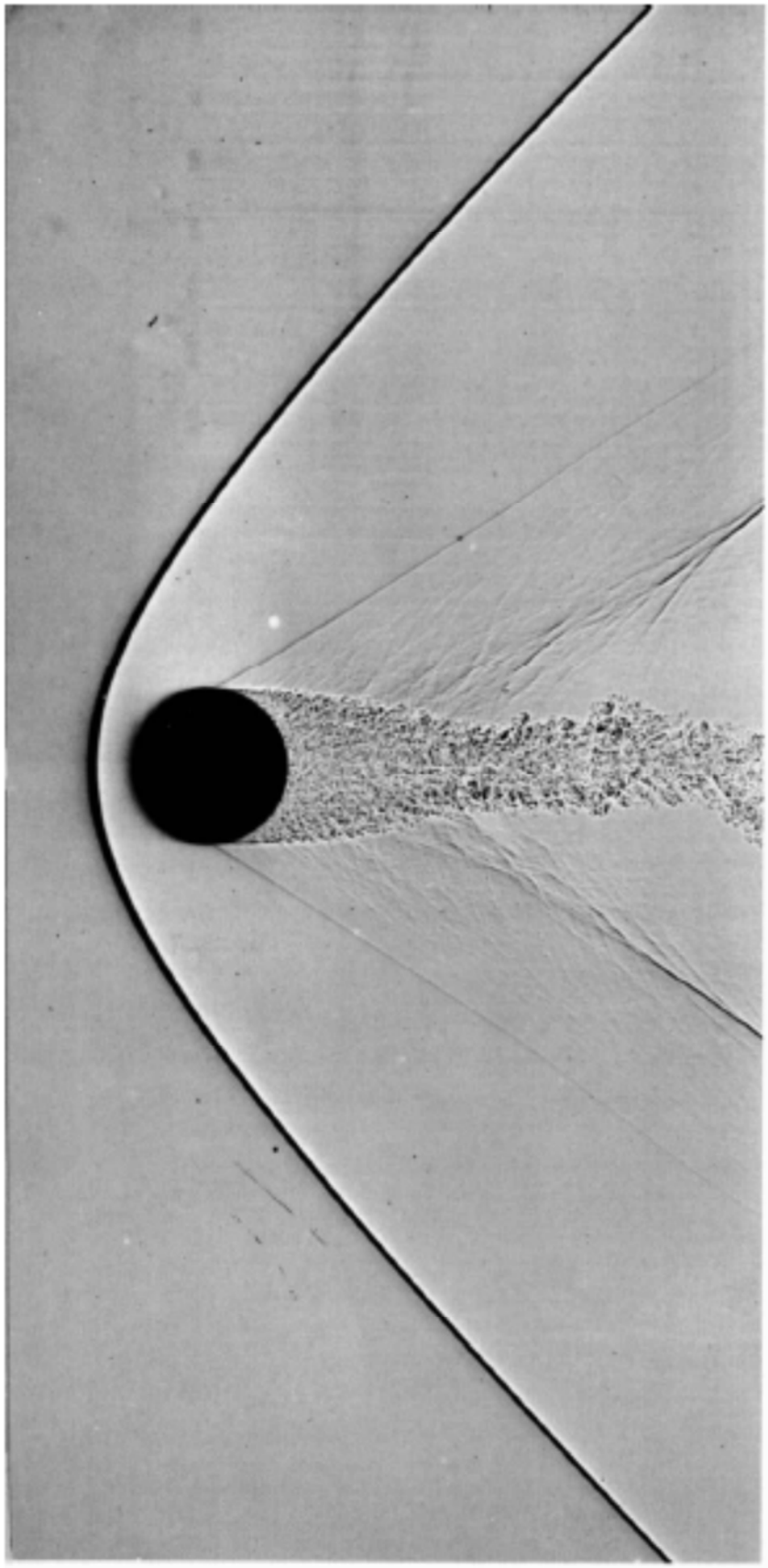

**266. Sphere at M = 1.53.** A shadowgraph catches a ½-inch sphere in free flight through air. The flow is subsonic behind the part of the bow wave that is ahead of the sphere, and over its surface back to 45°. At about 90° the laminar boundary layer separates through an oblique shock wave, and quickly becomes turbulent. The fluctuating wake generates a system of weak disturbances that merge into the second shock wave. *Photograph by A. C. Charters*